

Graphene-based tunable Bragg reflector with a broad bandwidth

Jin Tao^{1,3}, XueChao Yu¹, Bin Hu^{1,2}, Alexander Dubrovkin³ and Qi Jie Wang^{1,3},

¹ OPTIMUS, Photonics Centre of Excellence, School of Electrical and Electronic Engineering, Nanyang Technological University, 639798, Singapore

² School of Optoelectronics, Beijing Institute of Technology, Beijing, 100081, China

³ CDPT, Centre for Disruptive Photonic Technology, School of Physical and Mathematical Sciences, Nanyang Technological University, 639798, Singapore
qjwang@ntu.edu.sg

Abstract: We show theoretically that Bragg stopband and defect resonance mode can be achieved and dynamically tuned over a wide wavelength range by a small change in Fermi energy level of graphene, in graphene plasmonic waveguide structures.

OCIS codes: (130.3120) Integrated optics devices; (230.7370) Waveguides; (240.6680) Surface plasmons

1. Introduction

Graphene has attracted great interests due to its unique electronic and optical properties. High carrier mobility of graphene has been utilized in developing ultrafast photonic devices, such as the optical modulator [1], and photodetectors [2-3]. Graphene has also been found as a promising platform for plasmonic applications in the infrared frequency regimes. Much attention has been focused on localized graphene surface plasmon resonance with the incident light from free space, such as nanoribbons [4-5], nanodisks [6], and graphene-metal plasmonic antennas [7]. It is also interesting and indispensable to study the propagation properties of graphene plasmon waves.

In this work, we propose a plasmonic Bragg reflector structure formed in graphene waveguides and investigate its performance. We show that periodic stack of plasmonic graphene-silicon and graphene-air waveguides can be utilized to design effective filtering effects around Bragg wavelength. The tunability of the filtering stopband by electrostatic and defect cavity mode are also studied. In addition, we introduce a defect into the Bragg reflector to achieve a defect cavity mode formed in the stopband with a high-quality (high-Q) factor of 50. Such defect cavity microcavity may be used as graphene-based resonators for various applications.

2. Results

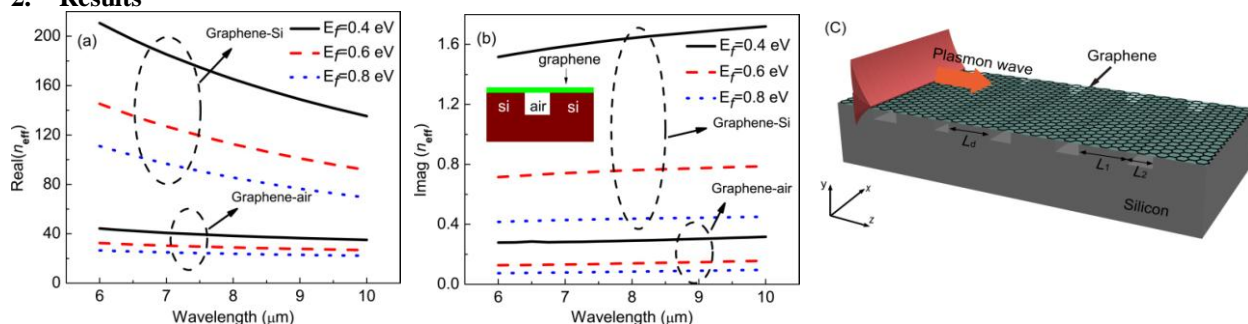


Fig. 1 (a) Real (n_{eff}), and (b) Imag (n_{eff}). The effective refractive index of a graphene plasmon mode at graphene-silicon waveguide and graphene-air waveguide as a function of optical wavelength for different Fermi energy levels. The depth of the air trench is 20 nm and the carrier mobility used is $\mu = 10000 \text{ cm}^2/(\text{V s})$. (c) Schematic of graphene plasmonic Bragg reflector formed in silicon grating substrate. The depth of air trench is 20 nm.

Figure 1 (a) shows the real part of effective refractive index of the surface plasmon mode supported by graphene sheet on silicon and air substrate for different Fermi energy levels. The effective refractive index at the Fermi energy level $E_f = 0.4 \text{ eV}$ is larger than 100, indicating that the mid-infrared plasmon wavelength is 2 orders of magnitude smaller than its wavelength in free space and the surface plasmon wave is highly localized. Imaginary part of effective refractive index of surface plasmon mode at different Fermi energy level is plotted in Fig. 1(b). As shown in Fig. 1 (a), there is a high effective index contrast for the surface plasmon mode between the graphene on silicon and air substrate. Thus, by periodically modulating the effective index along the graphene sheet which can be realized by alternatively stacking graphene-silicon and graphene-air waveguide, a Bragg reflector will be formed. Figure 1(c) shows the schematic of graphene plasmonic Bragg reflector formed in silicon gratings.

Fig. 2(a) shows the simulated transmission spectra of graphene plasmonic reflector with different Fermi energy levels. One can see that there are two wide stopbands with near-zero transmissions around the Bragg wavelength of

9.1 μm (corresponding to $m = 2$) and wavelength of 7.3 μm (corresponding to $m = 3$) for $E_f = 0.6$ eV which shows good filtering characteristics.

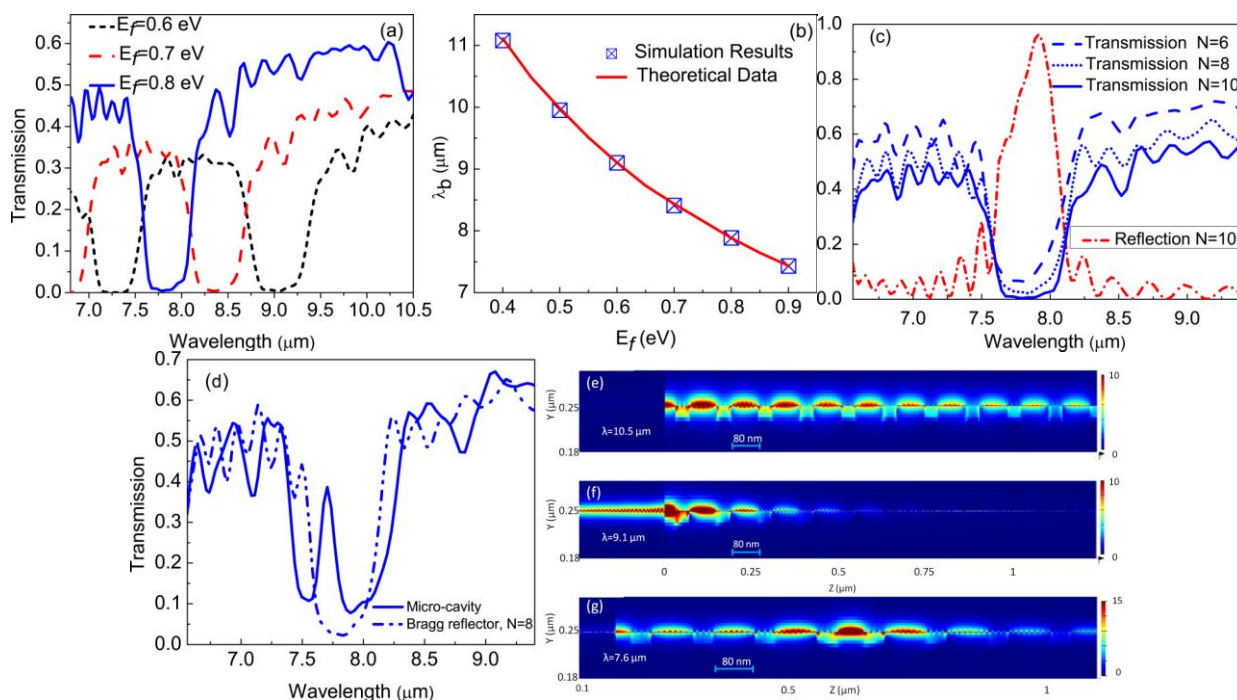


Fig. 2. (a) Simulated transmission spectra of graphene plasmonic reflector with different Fermi energy levels when $\mu = 10000$ $\text{cm}^2/(\text{V}\cdot\text{s})$. (b) Bragg wavelength as a function of Fermi energy level. The squares are simulated results from FDTD, and the red line is from theoretical calculations. The lengths of the graphene-silicon, graphene-air waveguide are $L_1 = 80$ nm, $L_2 = 40$ nm, respectively. The period of Bragg cell N is 10. (c) Transmission spectra of graphene Bragg reflector consisting of 6, 8 and 10 periods with Fermi energy level $E_f = 0.8$ eV, and reflection spectrum for periods of 10. (d) Transmission spectra of Bragg reflector with period number $N = 8$ and the microcavity formed by introducing a defect length $L_d = 50$ nm. (e) and (f) Simulated electric field intensity profiles of the plasmonic Bragg reflectors at the incident wavelength at 10.5 μm and 9.1 μm , and the structure parameters as the same as (a) with Fermi energy level of 0.6 eV. (g) Corresponds to the defect resonance mode in (d) at 7.6 μm .

Fig. 2(b) shows the central wavelength of Bragg reflector as a function of Fermi energy levels, which confirms the broad tuning range with a small change of Fermi level. The FDTD simulations results agree very well with the theoretical calculations. To further investigate the properties of the graphene plasmonic Bragg reflector, we introduce a defect into the graphene Bragg plasmonic structure by decreasing the length L_d of the central graphene-silicon waveguide. One can see a high Q defect resonance mode in Fig. 2 (d). Fig. 2(e-g) shows the field profiles of the graphene surface plasmon propagation through the Bragg reflector and the defect microcavity.

We expect graphene plasmonic Bragg reflector and defect mode resonance cavity will have great promise for the applications in building active integrated photonic integrated circuits.

This work is supported by the Ministry of Education, Singapore (MOE2011-T3-1-005).

Reference

- [1] M. Liu, X. B. Yin, E. Ulin-Avila, B. S. Geng, T. Zentgraf, L. Ju, F. Wang, and X. Zhang, "A graphene-based broadband optical modulator," *Nature* **474**, 64-67 (2011).
- [2] F. N. Xia, T. Mueller, Y. M. Lin, A. Valdes-Garcia, and P. Avouris, "Ultrafast graphene photodetector," *Nat Nanotechnol* **4**, 839-843 (2009).
- [3] Y. Zhang, T. Liu, B. Meng, G. Liang, X. Li, X. Hu, and Q. J. Wang, "Broadband high photoresponse from pure monolayer graphene photodetector," *Nat. Commun.* **4**, 1811-1822, 2013
- [4] V. W. Brar, M. S. Jang, M. Sherrott, J. J. Lopez, and H. A. Atwater, "Highly Confined Tunable Mid-Infrared Plasmonics in Graphene Nanoresonators," *Nano Lett* **13**, 2541-2547 (2013).
- [5] H. Yan, T. Low, W. Zhu, Y. Wu, M. Freitag, X. Li, F. Guinea, P. Avouris, and F. Xia, "Damping pathways of mid-infrared plasmons in graphene nanostructures," *Nat Photon* **7**, 394-399 (2013).
- [6] Z. Fang, S. Thongrattanasiri, A. Schlather, Z. Liu, L. Ma, Y. Wang, P. M. Ajayan, P. Nordlander, N. J. Halas, and F. J. Garcia de Abajo, "Gated Tunability and Hybridization of Localized Plasmons in Nanostructured Graphene," *ACS Nano* **7**, 2388-2395 (2013).
- [7] Y. Yao, M. A. Kats, P. Genevet, N. Yu, Y. Song, J. Kong, and F. Capasso, "Broad Electrical Tuning of Graphene-Loaded Plasmonic Antennas," *Nano Lett* **13**, 1257-1264 (2013).